

SLAC-PUB-8156
June 1999

Symmetry Tests in Polarized Z^0 Decays to $b\bar{b}g^*$

The SLD Collaboration**

Stanford Linear Accelerator Center

Stanford University, Stanford, CA 94309

ABSTRACT

Angular asymmetries have been measured in polarized Z^0 decays to $b\bar{b}g$ collected by the SLD experiment at the SLC. A high purity $b\bar{b}g$ event sample is selected by utilizing B lifetime information given by the SLD CCD pixel vertex detector and the stable micron-size SLC beams, and the b - and \bar{b} -jets are identified using lifetime information and momentum-weighted track charge. The forward-backward asymmetry is observed in the b -quark polar angle distribution, and the parity-violation parameter is measured to test the Standard Model. Two angular correlations between the three-jet plane and the Z^0 polarization are studied. The CP-even and T-odd, and the CP-odd and T-odd, angular asymmetries are sensitive to physics beyond the Standard Model. The latter requires tagging both the b - and \bar{b} -jet. We measure the expectation values of these quantities to be consistent with zero and set limits on the correlations at the 5% level.

Contributed to: the International Europhysics Conference on High Energy Physics, 15-21 July 1999, Tampere, Finland; Ref. 1-183, and to the XIXth International Symposium on Lepton and Photon Interactions, August 9-14 1999, Stanford, USA.

*Work supported by Department of Energy contract DE-AC03-76SF00515 (SLAC).

1. Introduction

The forward-backward polar-angle asymmetry in hadronic Z^0 decays to two jets has been investigated extensively at SLC and LEP to test the predictions of the electroweak theory of parity-violation in the $Z^0q\bar{q}$ coupling. In particular, at SLC where the electron beam is highly polarized, the left-right-forward-backward asymmetry removes the dependence on the $Z^0e^+e^-$ coupling and is directly sensitive to the $Z^0q\bar{q}$ coupling. The experimental results are found to be consistent with the theory to within experimental uncertainties of a few percent [1]. Hadronic Z^0 decays to three jets can be interpreted in terms of the fundamental process $Z^0 \rightarrow q\bar{q}g$ where one of the quarks has radiated a gluon. Given the success of the electroweak theory in predicting the two-jet polar-angle asymmetry, similar angular asymmetries can be measured in three-jet events to test Quantum Chromodynamics (QCD). The $Z^0 \rightarrow b\bar{b}g$ final state is particularly interesting as a search-ground for possible new physics processes beyond the Standard Model, and a high purity sample can be obtained with high efficiency due to the large mass and long lifetime of B-hadrons. Here we report the first experimental study of angular asymmetries in polarized Z^0 decays to $b\bar{b}g$.

2. Angular asymmetries in $Z^0 \rightarrow q\bar{q}g$

The differential cross section for $e^+e^- \rightarrow q\bar{q}g$ can be expressed as [2]

$$2\pi \frac{d^4\sigma}{d(\cos\theta)d\chi dx d\bar{x}} =$$
$$[\frac{3}{8}(1+\cos^2\theta)\frac{d^2\sigma_U}{dxd\bar{x}} + \frac{3}{4}\sin^2\theta\frac{d^2\sigma_L}{dxd\bar{x}} + \frac{3}{4}\sin^2\theta\cos2\chi\frac{d^2\sigma_T}{dxd\bar{x}} + \frac{3}{2\sqrt{2}}\sin2\theta\cos\chi\frac{d^2\sigma_I}{dxd\bar{x}}] h_f^{(1)}(s)$$
$$+ [\frac{3}{4}\cos\theta\frac{d^2\sigma_P}{dxd\bar{x}} - \frac{3}{\sqrt{2}}\sin\theta\cos\chi\frac{d^2\sigma_A}{dxd\bar{x}}] h_f^{(2)}(s), \quad (1)$$

where x and \bar{x} are the scaled momenta of the quark and anti-quark, respectively, θ is the polar angle of the thrust axis [3] w.r.t. the electron beam, and χ is the azimuthal angle of the event plane w.r.t. the quark-electron plane. Here the thrust axis is

defined so that it is parallel to the quark direction if the quark has the highest energy, and anti-parallel to the anti-quark direction if the anti-quark has the highest energy. The cross-section consists of six terms, each of which may be factorized into three contributions: 1) event orientation factor in terms of θ and χ ; 2) $d^2\sigma_i/dxd\bar{x}$ ($i=U,\dots,A$) determined by QCD; and 3) $h_f^{(1,2)}$ determined by the fermion electroweak couplings and beam polarization. While the first four terms are P-even, the last two terms are P-odd, and are sensitive to any parity-violating interactions at the $Z^0q\bar{q}$ and $gq\bar{q}$ vertices. In addition to these six terms, the most general differential cross section can have three more terms that are odd under time-reversal [4]. Being T-odd, however, these terms vanish at tree level in a theory that respects CPT invariance.

Recently Burrows and Osland have proposed new QCD tests in terms of the event orientation angles [5]. Integrating over scaled momenta and χ , the polar angle distribution of the thrust axis can be expressed as

$$\sigma(\cos\theta) \equiv \frac{d\sigma}{d\cos\theta} \propto (1 - P_{e^-} \cdot A_e)(1 + \alpha \cos^2\theta) + 2A_P(P_{e^-} - A_e)\cos\theta, \quad (2)$$

where A_P is the parity violation parameter:

$$A_P = \frac{\hat{\sigma}_P}{\hat{\sigma}_U + \hat{\sigma}_L} A_f. \quad (3)$$

Here $\alpha = \frac{\hat{\sigma}_U - 2\hat{\sigma}_L}{\hat{\sigma}_U + 2\hat{\sigma}_L}$, $\hat{\sigma}_i = \int \frac{d\sigma_i}{dxd\bar{x}} dx d\bar{x}$, and P_{e^-} is the signed electron beam polarization, and A_e (A_f) is the electroweak coupling of the Z^0 to the initial (final) state, given by $A_i = 2v_i a_i/(v_i^2 + a_i^2)$ in terms of the vector v_i and axial-vector a_i couplings. By manipulating the polarization sign of the electron beam the left-right-forward-backward asymmetry, \tilde{A}_{FB} , is directly sensitive to the asymmetry parameter A_P ,

$$\begin{aligned} \tilde{A}_{FB}(|\cos\theta|) &\equiv \frac{\sigma_L(|\cos\theta|) - \sigma_L(-|\cos\theta|) + \sigma_R(-|\cos\theta|) - \sigma_R(|\cos\theta|)}{\sigma_L(|\cos\theta|) + \sigma_L(-|\cos\theta|) + \sigma_R(-|\cos\theta|) + \sigma_R(|\cos\theta|)} \\ &= |P_e| A_P \frac{2|\cos\theta|}{1 + \cos^2\theta}. \end{aligned} \quad (4)$$

Similarly, by integrating over $\cos\theta$, x and \bar{x} , the azimuthal-angle distribution can be expressed as

$$2\pi \frac{d\sigma}{d\chi} \propto (1 - P_{e^-} \cdot A_e)(1 + \beta \cos 2\chi) - \frac{3\pi}{2\sqrt{2}} A'_P (P_{e^-} - A_e) \cos\chi, \quad (5)$$

where A'_P is the parity violation parameter:

$$A'_P = \frac{\hat{\sigma}_A}{\hat{\sigma}_U + \hat{\sigma}_L} A_f, \quad (6)$$

with $\beta = \frac{\hat{\sigma}_T}{\hat{\sigma}_U + \hat{\sigma}_L}$. Given the value of the electroweak parameter A_f , measurement of the angular asymmetry parameters A_P and A'_P in $Z^0 \rightarrow q\bar{q}g$ events allows one to test the QCD prediction for $\hat{\sigma}_P/(\hat{\sigma}_U + \hat{\sigma}_L)$ and $\hat{\sigma}_A/(\hat{\sigma}_U + \hat{\sigma}_L)$. Furthermore, the ratio A_P/A'_P is independent of A_f and is proportional to $\hat{\sigma}_A/\hat{\sigma}_P$.

The differential cross-section can also be expressed in terms of the polar angle ω of the vector \bar{n} normal to the event plane w.r.t. the electron beam direction, where $\cos \omega = \sin \theta \sin \chi$:

$$\frac{d\sigma}{d \cos \omega} \propto (1 - P_{e^-} \cdot A_e)(1 + \gamma \cos^2 \omega) + \frac{16}{9} A_T (P_{e^-} - A_e) \cos \omega, \quad (7)$$

with $\gamma = -\frac{1}{3} \frac{\hat{\sigma}_U - 2\hat{\sigma}_L + 6\hat{\sigma}_T}{\hat{\sigma}_U + 2/3\hat{\sigma}_L + 2/3\hat{\sigma}_T}$. At first order in perturbative QCD, $\hat{\sigma}_L = 2\hat{\sigma}_T$, yielding $\gamma = -\frac{1}{3}$, and $A_T = 0$. The second term is one of the three T-odd terms mentioned above, and appears as a forward-backward asymmetry of the event-plane normal relative to the Z^0 polarization axis. The left-right-forward-backward asymmetry in $\cos \omega$ can also be defined by a similar double asymmetry as Eq. 4, and is directly proportional to the T-odd parameter A_T . The vector normal to the event plane can be defined in two ways: 1) the three jets are ordered according to their energies, and the two highest energy jet momenta are used to define $\bar{n} = \vec{p}_1 \times \vec{p}_2$; and 2) the quark and anti-quark momenta are used to define $\bar{n} = \vec{p}_q \times \vec{p}_{\bar{q}}$. The asymmetry term is CP-even in the first definition, and CP-odd in the second. The first definition does not require jet flavor identification, and we have studied the asymmetry for inclusive hadronic Z^0 decays [6]. The second definition requires tagging both quark- and antiquark-jets. In both cases, in the Standard Model the asymmetry vanishes identically at tree level, but higher-order processes yield non-zero contributions for $e^+e^- \rightarrow b\bar{b}g$. However, due to various cancellations, these contributions are found to be very small at the Z^0 resonance and yield values of the asymmetry parameter $|A_T| < 10^{-5}$ [7]. Measurement

of the asymmetry in $\cos \omega$ is hence potentially sensitive to physics processes beyond the Standard Model [8].

3. Event and Track Selection

The SLAC Linear Collider (SLC) collides longitudinally polarized electrons with unpolarized positrons at a center-of-mass energy of 91.2 GeV. The electron polarization direction is randomly reversed pulse-by-pulse, reducing systematic effects on polarization-dependent asymmetries. The magnitude of the average electron-beam polarization was 0.63 in 1993, 0.77 in 1994-1996, and 0.73 in 1997-1998.

The measurement was performed with the SLC Large Detector (SLD) using approximately 550,000 Z^0 decays collected between 1993 and 1998. A general description of the SLD can be found elsewhere [9]. Charged particle tracking and momentum analysis is provided by the central drift chamber (CDC) [10] and the CCD-based vertex detector (VXD) [11] in a uniform axial magnetic field of 0.6 T. About 70% of the data were taken with a new vertex detector (VXD3) installed in 1996, and the rest with the previous detector, VXD2. Particle energies are measured in the liquid argon calorimeter (LAC) [12] and in the warm iron calorimeter [13].

In the present analysis the hadronic event selection, three-jet reconstruction, and b-tagging were based on charged tracks. A set of cuts was applied to the data to select well-measured tracks and events well contained within the detector acceptance [14]. Events were required to have (i) at least 7 charged tracks; (ii) a visible charged energy of at least 20 GeV; and (iii) a thrust axis [3] polar angle satisfying $|\cos \theta_T| < 0.71$, which was reconstructed using the LAC. Charged tracks reconstructed in the CDC were linked with pixel clusters in the VXD by extrapolating each track and selecting the best set of associated clusters. The average efficiency of reconstruction in the CDC and linking to the correct set of VXD hits is 95% (94%) for the region $|\cos \theta| < 0.85$ (0.74) [15]. The momentum resolution of the combined CDC and VXD systems

is $(\delta p_\perp/p_\perp)^2 = (.01)^2 + (.0026p_\perp)^2$, where p_\perp is the transverse momentum in GeV/c w.r.t. the beamline.

The centroid of the micron-size SLC Interaction Point (IP) in the $r\phi$ plane is reconstructed with a measured precision of $\sigma_{r\phi}^{IP} \sim 5\mu\text{m}$ ($7\mu\text{m}$) using tracks in sets of ≈ 30 sequential hadronic Z^0 decays. The z position of the IP is determined on an event-by-event basis with a precision of $\sigma_z^{IP} \sim 32\mu\text{m}$ ($52\mu\text{m}$) using the median z position of tracks at their point-of-closest approach to the IP in the $r\phi$ plane. The track impact parameter resolution at high momentum is $11\mu\text{m}$ ($11\mu\text{m}$) in the plane perpendicular to the beam axis ($r\phi$ plane) and $23\mu\text{m}$ ($38\mu\text{m}$) in the plane containing the beam axis (rz plane).

A set of “quality” tracks for use in heavy quark tagging was selected. Tracks measured in the CDC were required to have ≥ 40 hits, with the first hit at a radius $r < 39$ cm, a transverse momentum $p_\perp > 0.4$ GeV/c , a good fit quality ($\chi^2/N_{DOF} < 5$), and to extrapolate to the IP within 1 cm in $r\phi$ and 1.5 cm in z . Tracks were required to have at least one associated VXD hit, and a combined CDC-VXD fit with $\chi^2/N_{DOF} < 5$. Tracks with an $r\phi$ impact parameter $\delta > 3$ mm or with an impact parameter error $\sigma_\delta > 250\mu\text{m}$ were removed. Tracks from identified γ conversions and K^0 or Λ^0 decays were also removed.

4. $b\bar{b}g$ Analysis

Three-jet events were selected and the three momentum vectors of the jets were reconstructed. Although the parton momenta are not directly measurable, at $\sqrt{s} \approx 91$ GeV the partons usually appear as well-collimated jets of hadrons. Jets were reconstructed using the “Durham” jet algorithm [16]. Planar three-jet events were selected by requiring exactly three reconstructed jets to be found with a jet-resolution parameter value of $y_c=0.005$, the sum of the angles between the three jets to be greater than 358° , and that each jet contain at least two charged tracks. A total of 75,000 events satisfied

these criteria.

Such jet algorithms accurately reconstruct the parton directions but measure the parton energies poorly [17]. Therefore, the jet energies were calculated by using the measured jet directions and solving the three-body kinematics assuming massless jets, and were then used to label the jets such that $E_1 > E_2 > E_3$. The energy of jet 1, for example, is given by

$$E_1 = \sqrt{s} \frac{\sin \theta_{23}}{\sin \theta_{12} + \sin \theta_{23} + \sin \theta_{31}}, \quad (8)$$

where θ_{kl} is the angle between jets k and l .

To select $b\bar{b}g$ events the long lifetime and large invariant mass of B-hadrons was exploited. A topological algorithm [18] was applied to the set of quality tracks in each jet to search for a secondary decay vertex. Vertices were required to be separated from the IP by at least 1 mm and to contain at least two tracks. Monte Carlo studies show that the probability for reconstructing at least one such vertex was $\sim 91\%$ (77%) in $b\bar{b}g$ events, $\sim 45\%$ (26%) in $c\bar{c}g$ events, and $\sim 2\%$ (2%) in light quark events. Once a vertex was found, additional tracks consistent with coming from the vertex were attached in an attempt to reconstruct the invariant mass of a B-hadron. A vertex axis was formed by a straight line joining the IP and the vertex, which was located at a distance D from the IP. For each quality track the distance of closest approach, T , and the distance from the IP along the vertex axis to the point of closest approach, L , were calculated. Tracks with $T < 1$ mm, and $L/D > 0.25$ were attached to the secondary vertex, and the vertex invariant mass, M_{ch} , was calculated assuming each track was a charged pion. Due to neutral decay products the total momentum vector of the tracks and the vertex axis were typically acollinear. To account for the missing neutral particles, an additional component of transverse momentum P_t , defined by the projection of the total momentum vector perpendicular to the vertex axis, was added to yield $M = \sqrt{M_{ch}^2 + P_t^2} + |P_t|$ [19]. Figures 1(a), (b), and (c) show the distributions of this P_t -corrected vertex mass for jet 1, 2, and 3, respectively. An event

was selected as $b\bar{b}g$ if at least one jet contained a vertex with $M > 1.5 \text{ GeV}/c^2$. A total of 14,658 events satisfied this requirement and were subjected to further analysis. Monte Carlo studies show that this selection is 84% (69%) efficient for identifying a sample of $b\bar{b}g$ events with 84% (87%) purity, and containing 14% (11%) $c\bar{c}g$ and 2% (2%) light-flavor backgrounds.

The identification of each jet was based on the momentum-weighted jet charge and $r\phi$ impact parameter techniques. The momentum-weighted charge was calculated for each jet:

$$Q_j = \sum q_i |\vec{p}_i \cdot \vec{\hat{t}}|^\kappa, \quad (9)$$

where $\kappa=0.5$, $\vec{\hat{t}}$ is the unit vector along the event thrust axis, and q_i and \vec{p}_i are the charge and momentum of the i^{th} track associated with jet j . We then examined the difference in the momentum-weighted jet charge, $Q_{diff} = Q_1 - Q_2 - Q_3$. If this quantity was negative (positive), jet 1 was tagged as the b-jet (\bar{b} -jet). The jet flavor was tagged by counting the number of “significant” tracks with normalized impact parameter w.r.t the IP $d/\sigma_d > 3$. Figures 2(a), (b), and (c) show the distributions of the number of significant tracks found in jets 1, 2, and 3, respectively, in the b-tagged events. Jet 1 was chosen as the gluon-jet only if jet 1 had no significant track and both jet 2 and 3 had at least one significant track. Jet 2 was chosen as the gluon-jet if jet 2 had no significant track and jet 3 had at least one significant track. Otherwise, jet 3 was chosen as the gluon-jet.

5. Monte Carlo Simulation

A Monte Carlo simulation of hadronic Z^0 decays combined with a simulation of the detector response was used to study the quality of the jet reconstruction, the b-tagging efficiency and purity, and the efficiency of the jet flavor identification. The JETSET 7.4 [20] event generator was used, with parameter values tuned to hadronic e^+e^- annihilation data [21], combined with a simulation of B hadron decays tuned [22]

to $\Upsilon(4S)$ data and a detector simulation based on GEANT 3.21 [23]. For those events satisfying the three-jet criteria, exactly three jets were reconstructed at the parton level by applying the jet algorithm to the parton momenta. The three parton-level jets were associated with the three detector-level jets by choosing the combination that minimized the sum of the angular differences between the corresponding jets, and the energies and charges of the matching jets were compared.

For the T-odd asymmetry analyses the vector normal to the jet plane is measured in two ways: 1) using the two highest energy jets, and 2) using identified b - and \bar{b} -jets. In the first method, where the jets are labeled according to their energy, six detector-jet energy orderings are possible for a given parton-jet energy ordering. For the three cases where the energy ordering of any two jets does not agree between parton and detector levels, the direction of the jet-plane normal vector is opposite between the parton level and detector level and $\cos\omega$ will be measured with the wrong sign. The average probability of measuring $\cos\omega$ with the correct sign in this analysis is estimated from the simulation to be 76% (76%). In the second method, where both b - and \bar{b} -jets are identified, the gluon-jet must be tagged correctly, and furthermore, the charge assignment of the b - and \bar{b} -jets must be correct. The average probability of identifying the gluon-jet correctly is 91% (88%), and combined with the correct-charge assignment probability determined by the self-calibration technique described in the next section, the average probability of measuring $\cos\omega$ with the right sign is 64% (63%).

6. Angular Asymmetries

Figures 3(a) and (b) show the observed $\cos\theta$ distributions of the signed-thrust axis for event samples collected with left- and right-handed electron beam, respectively. The histograms show the backgrounds estimated using the simulation. The thrust axis is signed so that it points towards the hemisphere containing the b -tagged jet. The $\cos\theta$ distribution may be described by

$$\begin{aligned}
\frac{d\sigma}{d\cos\theta} = & (1 - P_{e^-} \cdot A_e)(1 + \alpha \cos^2\theta) + \\
& 2(P_{e^-} - A_e) \cos\theta [A_{P,b} f_b (2p^{correct,b} - 1) + \\
& A_{P,c} f_c (2p^{correct,c} - 1) + A_{P,uds} (1 - f_b - f_c) (2p^{correct,uds} - 1)], \quad (10)
\end{aligned}$$

where f_b , f_c , f_{uds} are the fractions of $b\bar{b}g$, $c\bar{c}g$, and light quark events in the sample, determined from the Monte Carlo simulation, and $p^{correct,b}$, $p^{correct,c}$, $p^{correct,uds}$ are the probabilities to tag the parton charge correctly for $b\bar{b}g$, $c\bar{c}g$, and the light quark events, respectively. The correct-charge probability is calculated as a function of the measured jet charge difference $|Q_{diff}|$ as $p^{correct} = 1/(1 + e^{-\alpha|Q_{diff}|})$. The quantity α is a parametrization of how well the momentum-weighted charge technique signs the thrust axis direction. While α_c and α_{uds} for $c\bar{c}g$ and light-quark backgrounds were calculated from the simulation, α_b for $b\bar{b}g$ events was determined from data using a self-calibration technique [24]. Using the measured widths, σ_{diff} and σ_{sum} , of the Q_{diff} ($= Q_1 - Q_2 - Q_3$) and Q_{sum} ($= Q_1 + Q_2 + Q_3$) distributions:

$$\alpha_b = \frac{2\sqrt{\sigma_{diff}^2 - (1 + \lambda)^2\sigma_{sum}^2}}{(1 + \lambda)^2\sigma_{sum}^2}, \quad (11)$$

where the hemisphere correlation $\lambda = 0.027$ was calculated from the simulation. This yielded $\alpha_b = 0.218 \pm 0.021$ (0.255 ± 0.032) averaged over $\cos\theta$. On average the correct-charge assignment probability for $b\bar{b}g$ events is 68% (67%). The asymmetry parameters $A_{P,c}$ and $A_{P,uds}$ (Eq. 3) for charm and light-quark backgrounds were calculated from the simulation based on the Standard Model. A maximum-likelihood fit of Eq. 10 is performed to extract $A_{P,b}$. We found

$$A_{P,b} = 0.847 \pm 0.049, \quad (PRELIMINARY) \quad (12)$$

where the error is statistical only. Assuming the Standard Model expectation of $A_b = 0.94$ for $\sin^2\theta_w = 0.23$, the measured value of $A_{P,b}$ yields

$$\frac{\hat{\sigma}_P}{\hat{\sigma}_U + \hat{\sigma}_L} = 0.906 \pm 0.052(stat.).$$

This value is consistent with the $\mathcal{O}(\alpha_s^2)$ QCD expectation of $\hat{\sigma}_P/(\hat{\sigma}_U + \hat{\sigma}_L) = 0.93$, calculated using the JETSET 7.4 event generator [20].

Figures 4(a) and (b) show the χ distributions for event samples collected with left- and right-handed electron beam, respectively. The χ distribution may be described by

$$\begin{aligned} \frac{d\sigma}{d\chi} = & (1 - P_{e^-} \cdot A_e)(1 + \beta \cos 2\chi) - \\ & \frac{3\pi}{2\sqrt{2}} (P_{e^-} - A_e) \cos \chi [A'_{P,b} f_b P_{AP}^b + \\ & A'_{P,c} f_c P_{AP}^c + A'_{P,uds} (1 - f_b - f_c) P_{AP}^{uds}], \end{aligned} \quad (13)$$

where P_{AP}^b , P_{AP}^c , and P_{AP}^{uds} are the analyzing powers for $b\bar{b}g$, $c\bar{c}g$, and light quark events, respectively, and are function of the probability to tag the parton charge correctly, P_{chg} , and the probability to tag the gluon-jet correctly, P_{glu} , given by

$$P_{AP} = P_{chg}P_{glu} - (1 - P_{chg})P_{glu} - P_{chg}(1 - P_{glu}) + (1 - P_{chg})(1 - P_{glu}). \quad (14)$$

A maximum-likelihood fit of Eq. 13 is performed to extract $A'_{P,b}$. We found

$$A'_{P,b} = -0.013 \pm 0.033, \quad (\text{PRELIMINARY}) \quad (15)$$

where the error is statistical only. Assuming the Standard Model expectation of $A_b = 0.94$ for $\sin^2 \theta_w = 0.23$, the measured value of $A'_{P,b}$ yields

$$\frac{\hat{\sigma}_A}{\hat{\sigma}_U + \hat{\sigma}_L} = -0.014 \pm 0.035(\text{stat.}).$$

This value is consistent with the $\mathcal{O}(\alpha_s^2)$ QCD expectation of $\hat{\sigma}_A/(\hat{\sigma}_U + \hat{\sigma}_L) = -0.064$, calculated using the JETSET 7.4 event generator [20].

Figures 5(a) and (b) show the left-right-forward-backward asymmetry of the $\cos \omega$ distribution for the two definitions: (a) $\vec{p}_1 \times \vec{p}_2$, and (b) $\vec{p}_b \times \vec{p}_{\bar{b}}$. No asymmetry is apparent. The $\cos \omega$ distribution may be described, assuming no asymmetries in the $c\bar{c}g$ and light-quark backgrounds, by

$$\frac{d\sigma}{d\cos\omega} \propto (1 - P_{e^-} \cdot A_e)(1 - \frac{1}{3}\cos^2\omega) + \frac{16}{9}(P_{e^-} - A_e)A_T f_b P_{AP} \cos\omega, \quad (16)$$

where f_b is the fraction of $b\bar{b}g$ events in the sample, and the analyzing power, P_{AP} , represents the probability of correctly signing the vector normal to the event plane. In the first case P_{AP} is given by the probability of correct energy-ordering, $P_{AP} = (2p^{correct} - 1)$, and in the second case it is the probability of correct-sign assignment combined with the tagging efficiency of the gluon-jet. We performed maximum-likelihood fits of Eq. 16 to the $\cos\omega$ distributions to extract the parameters A_T^+ , for the CP-even case, and A_T^- , for the CP-odd case.

We found

$$A_T^+ = -0.012 \pm 0.013, \quad (PRELIMINARY)$$

$$A_T^- = -0.033 \pm 0.023, \quad (PRELIMINARY)$$

where the error is statistical only. In both cases the T-odd contribution is consistent with zero within the statistical error and we calculate limits of

$$-0.038 < A_T^+ < 0.014 \quad @ \quad 95\% \quad C.L., \quad (PRELIMINARY)$$

$$-0.077 < A_T^- < 0.011 \quad @ \quad 95\% \quad C.L.. \quad (PRELIMINARY)$$

The results of these fits are shown in Figures 5(a) and 5(b).

7. Systematic Errors

Table 1 summarizes the systematic errors on the forward-backward asymmetry analysis of the signed thrust-axis. The largest systematic error was due to the statistical uncertainty in the α_b determination using the self-calibration technique. This error would decrease with a larger data sample. The systematic error in the inter-hemisphere correlation λ was due to the limited statistics of the Monte Carlo simulation. The

systematic error in the tag composition was due to the heavy quark physics modeling. In $b\bar{b}$ events we have considered the uncertainties on: the branching fraction for $Z^0 \rightarrow b\bar{b}$, the B hadron fragmentation function, the rates of production of B^\pm , B^0 and B_s^0 mesons, and B baryons, the lifetimes of B mesons and baryons, and the average B hadron decay charge multiplicity. In $c\bar{c}$ events we have considered the uncertainties on: the branching fraction for $Z^0 \rightarrow c\bar{c}$, the charmed hadron fragmentation function, the rates of production of D^0 , D^+ and D_s mesons, and charmed baryons, and the charged multiplicity of charmed hadron decays. We have also considered the rate of production of $s\bar{s}$ in the jet fragmentation process, and the production of secondary $b\bar{b}$ and $c\bar{c}$ from gluon splitting. The systematic error in the detector modeling results from discrepancies between data and Monte Carlo in tracking efficiency and resolution. The systematic errors on A'_P and A_T are negligibly small as the uncertainty diminishes with the asymmetry itself.

8. Conclusions

In conclusion, we have made the first angular asymmetry measurements in polarized Z^0 decays to $b\bar{b}g$. From the forward-backward polar angle asymmetry of the signed-thrust axis we have measured the parity violation parameter $A_P = 0.847 \pm 0.049$ (stat.) ± 0.060 (syst.). From the azimuthal angle asymmetry we have measured the second parity violation parameter $A'_P = -0.013 \pm 0.033$ (stat.) ± 0.002 (syst.). Assuming the Standard Model expectation of $A_b = 0.94$, the QCD factors for $b\bar{b}g$ events are measured to be $\hat{\sigma}_P/(\hat{\sigma}_U + \hat{\sigma}_L) = 0.906 \pm 0.052$ (stat.) ± 0.064 (syst.), and $\hat{\sigma}_A/(\hat{\sigma}_U + \hat{\sigma}_L) = -0.014 \pm 0.035$ (stat.) ± 0.002 (syst.), which are consistent with the $\mathcal{O}(\alpha_s^2)$ QCD expectations. We find the T-odd asymmetry to be consistent with zero, and we set 95% C.L. limits on the asymmetry parameter $-0.038 < A_T^+ < 0.014$ for the CP-even case and $-0.077 < A_T^- < 0.011$ for the CP-odd case. All results are preliminary.

Acknowledgements

We thank the personnel of the SLAC accelerator department and the technical staffs of our collaborating institutions for their outstanding efforts on our behalf.

*Work supported by Department of Energy contracts: DE-FG02-91ER40676 (BU), DE-FG03-91ER40618 (UCSB), DE-FG03-92ER40689 (UCSC), DE-FG03-93ER40788 (CSU), DE-FG02-91ER40672 (Colorado), DE-FG02-91ER40677 (Illinois), DE-AC03-76SF00098 (LBL), DE-FG02-92ER40715 (Massachusetts), DE-FC02-94ER40818 (MIT), DE-FG03-96ER40969 (Oregon), DE-AC03-76SF00515 (SLAC), DE-FG05-91ER40627 (Tennessee), DE-FG02-95ER40896 (Wisconsin), DE-FG02-92ER40704 (Yale); National Science Foundation grants: PHY-91-13428 (UCSC), PHY-89-21320 (Columbia), PHY-92-04239 (Cincinnati), PHY-95-10439 (Rutgers), PHY-88-19316 (Vanderbilt), PHY-92-03212 (Washington); The UK Particle Physics and Astronomy Research Council (Brunel, Oxford and RAL); The Istituto Nazionale di Fisica Nucleare of Italy (Bologna, Ferrara, Frascati, Pisa, Padova, Perugia); The Japan-US Cooperative Research Project on High Energy Physics (Nagoya, Tohoku); The Korea Research Foundation (Soongsil, 1997).

References

- [1] K. Abe *et al.*, Phys. Rev. Lett. **81**, 942 (1998) and references therein.
- [2] H. A. Olsen *et al.*, Nucl. Phys. **B171**, 209 (1980).
- [3] S. Brandt *et al.*, Phys. Lett. **12**, 57 (1964), and E. Farhi, Phys. Rev. Lett. **39**, 1587 (1977).
- [4] K. Hagiwara *et al.*, Nucl. Phys. **B358**, 80 (1991).
- [5] P. N. Burrows and P. Osland, Phys. Lett. **B400**, 385 (1997).
- [6] K. Abe *et al.*, Phys. Rev. Lett. **75**, 4173 (1996).
- [7] A. Brandenburg, L. Dixon, and Y. Shadmi, Phys. Rev. **D53**, 1264 (1996).
- [8] See, for example, C. D. Carone and H. Murayama, Phys. Rev. Lett. **74**, 3122 (1995).

- [9] SLD Design Report, SLAC Report 273 (1984).
- [10] M. D. Hildreth *et al.*, Nucl. Inst. Meth. **A367**, 111 (1995)
- [11] C. J. S. Damerell *et al.*, Nucl. Inst. Meth. **A288**, 236 (1990), and K. Abe *et al.*, Nucl. Inst. Meth. **A400**, 287 (1997).
- [12] D. Axen *et. al.*, Nucl. Inst. Meth. **A238**, 472 (1993).
- [13] A. C. Benvenuti *et al.*, Nucl. Inst. Meth. **A290**, 353 (1990).
- [14] K. Abe *et al.*, Phys. Rev. **D51**, 962 (1995).
- [15] The values correspond to the VXD3 data set taken in 1996-1998, while the values in parentheses to the VXD2 data taken in 1993-1995.
- [16] S. Catani *et al.*, Phys. Lett. **B263**, 491 (1991).
- [17] R. Brandelik *et al.*, Phys. Lett. **B97**, 453 (1980), B. Adeva *et al.*, Phys. Lett. **263**, 551 (1991); and G. Alexander *et al.*, Z. Phys. **C52**, 543 (1991).
- [18] D. J. Jackson, Nucl. Inst. Meth. **A388**, 247 (1997).
- [19] The missing momentum is calculated by taking into account the measurement resolution of the primary and secondary vertices. We further restrict M to be $\leq 2 \times M_{ch}$ to reduce contaminations from fake vertices in light quark events.
- [20] T. Sjöstrand, Computer Phys. Commun. **82** 74 (1994).
- [21] P. N. Burrows, Z. Phys. **C41**, 375 (1988), and OPAL Collab., M. Z. Akrawy *et al.*, Z. Phys. **C47**, 505 (1990).
- [22] SLD Collab., K. Abe *et al.*, SLAC-PUB-7117 (to appear in Phys. Rev. Lett.).
- [23] R. Brun *et al.*, Report No. CERN-DD/EE/84-1 (1989).

[24] T. Junk, Stanford Univ. Ph. D thesis, SLAC-Report-476, (1995) (unpublished), and V. Serbo, Univ. of Wisconsin Ph. D thesis, SLAC-Report-510, (1997) (unpublished).

**List of Authors

Kenji Abe,⁽²¹⁾ Koya Abe,⁽³³⁾ T. Abe,⁽²⁹⁾ I. Adam,⁽²⁹⁾ T. Akagi,⁽²⁹⁾ N. J. Allen,⁽⁵⁾ W.W. Ash,⁽²⁹⁾ D. Aston,⁽²⁹⁾ K.G. Baird,⁽¹⁷⁾ C. Baltay,⁽⁴⁰⁾ H.R. Band,⁽³⁹⁾ M.B. Barakat,⁽¹⁶⁾ O. Bardon,⁽¹⁹⁾ T.L. Barklow,⁽²⁹⁾ G. L. Bashindzhagyan,⁽²⁰⁾ J.M. Bauer,⁽¹⁸⁾ G. Bellodi,⁽²³⁾ R. Ben-David,⁽⁴⁰⁾ A.C. Benvenuti,⁽³⁾ G.M. Bilei,⁽²⁵⁾ D. Bisello,⁽²⁴⁾ G. Blaylock,⁽¹⁷⁾ J.R. Bogart,⁽²⁹⁾ G.R. Bower,⁽²⁹⁾ J. E. Brau,⁽²²⁾ M. Breidenbach,⁽²⁹⁾ W.M. Bugg,⁽³²⁾ D. Burke,⁽²⁹⁾ T.H. Burnett,⁽³⁸⁾ P.N. Burrows,⁽²³⁾ A. Calcaterra,⁽¹²⁾ D. Calloway,⁽²⁹⁾ B. Camanzi,⁽¹¹⁾ M. Carpinelli,⁽²⁶⁾ R. Cassell,⁽²⁹⁾ R. Castaldi,⁽²⁶⁾ A. Castro,⁽²⁴⁾ M. Cavalli-Sforza,⁽³⁵⁾ A. Chou,⁽²⁹⁾ E. Church,⁽³⁸⁾ H.O. Cohn,⁽³²⁾ J.A. Coller,⁽⁶⁾ M.R. Convery,⁽²⁹⁾ V. Cook,⁽³⁸⁾ R. Cotton,⁽⁵⁾ R.F. Cowan,⁽¹⁹⁾ D.G. Coyne,⁽³⁵⁾ G. Crawford,⁽²⁹⁾ C.J.S. Damerell,⁽²⁷⁾ M. N. Danielson,⁽⁸⁾ M. Daoudi,⁽²⁹⁾ N. de Groot,⁽⁴⁾ R. Dell'Orso,⁽²⁵⁾ P.J. Dervan,⁽⁵⁾ R. de Sangro,⁽¹²⁾ M. Dima,⁽¹⁰⁾ A. D'Oliveira,⁽⁷⁾ D.N. Dong,⁽¹⁹⁾ M. Doser,⁽²⁹⁾ R. Dubois,⁽²⁹⁾ B.I. Eisenstein,⁽¹³⁾ V. Eschenburg,⁽¹⁸⁾ E. Etzion,⁽³⁹⁾ S. Fahey,⁽⁸⁾ D. Falciai,⁽¹²⁾ C. Fan,⁽⁸⁾ J.P. Fernandez,⁽³⁵⁾ M.J. Fero,⁽¹⁹⁾ K. Flood,⁽¹⁷⁾ R. Frey,⁽²²⁾ J. Gifford,⁽³⁶⁾ T. Gillman,⁽²⁷⁾ G. Gladding,⁽¹³⁾ S. Gonzalez,⁽¹⁹⁾ E. R. Goodman,⁽⁸⁾ E.L. Hart,⁽³²⁾ J.L. Harton,⁽¹⁰⁾ A. Hasan,⁽⁵⁾ K. Hasuko,⁽³³⁾ S. J. Hedges,⁽⁶⁾ S.S. Hertzbach,⁽¹⁷⁾ M.D. Hildreth,⁽²⁹⁾ J. Huber,⁽²²⁾ M.E. Huffer,⁽²⁹⁾ E.W. Hughes,⁽²⁹⁾ X. Huynh,⁽²⁹⁾ H. Hwang,⁽²²⁾ M. Iwasaki,⁽²²⁾ D. J. Jackson,⁽²⁷⁾ P. Jacques,⁽²⁸⁾ J.A. Jaros,⁽²⁹⁾ Z.Y. Jiang,⁽²⁹⁾ A.S. Johnson,⁽²⁹⁾ J.R. Johnson,⁽³⁹⁾ R.A. Johnson,⁽⁷⁾ T. Junk,⁽²⁹⁾ R. Kajikawa,⁽²¹⁾ M. Kalelkar,⁽²⁸⁾ Y. Kamyshkov,⁽³²⁾ H.J. Kang,⁽²⁸⁾ I. Karliner,⁽¹³⁾ H. Kawahara,⁽²⁹⁾ Y. D. Kim,⁽³⁰⁾ M.E. King,⁽²⁹⁾ R. King,⁽²⁹⁾ R.R. Kofler,⁽¹⁷⁾ N.M. Krishna,⁽⁸⁾ R.S. Kroeger,⁽¹⁸⁾ M. Langston,⁽²²⁾ A. Lath,⁽¹⁹⁾ D.W.G. Leith,⁽²⁹⁾ V. Lia,⁽¹⁹⁾ C. Lin,⁽¹⁷⁾ M.X. Liu,⁽⁴⁰⁾ X. Liu,⁽³⁵⁾ M. Loretta,⁽²⁴⁾ A. Lu,⁽³⁴⁾ H.L. Lynch,⁽²⁹⁾ J. Ma,⁽³⁸⁾ G. Mancinelli,⁽²⁸⁾ S. Manly,⁽⁴⁰⁾ G. Mantovani,⁽²⁵⁾ T.W. Markiewicz,⁽²⁹⁾ T. Maruyama,⁽²⁹⁾ H. Masuda,⁽²⁹⁾ E. Mazzucato,⁽¹¹⁾ A.K. McKemey,⁽⁵⁾ B.T. Meadows,⁽⁷⁾ G. Menegatti,⁽¹¹⁾ R. Messner,⁽²⁹⁾ P.M. Mockett,⁽³⁸⁾ K.C. Moffeit,⁽²⁹⁾ T.B. Moore,⁽⁴⁰⁾ M. Morii,⁽²⁹⁾ D. Muller,⁽²⁹⁾ V. Murzin,⁽²⁰⁾ T. Nagamine,⁽³³⁾ S. Narita,⁽³³⁾ U. Nauenberg,⁽⁸⁾ H. Neal,⁽²⁹⁾ M. Nussbaum,⁽⁷⁾ N. Oishi,⁽²¹⁾ D. Onoprienko,⁽³²⁾ L.S. Osborne,⁽¹⁹⁾ R.S. Panvini,⁽³⁷⁾

C. H. Park,⁽³¹⁾ T.J. Pavel,⁽²⁹⁾ I. Peruzzi,⁽¹²⁾ M. Piccolo,⁽¹²⁾ L. Piemontese,⁽¹¹⁾
 K.T. Pitts,⁽²²⁾ R.J. Plano,⁽²⁸⁾ R. Prepost,⁽³⁹⁾ C.Y. Prescott,⁽²⁹⁾ G.D. Punkar,⁽²⁹⁾
 J. Quigley,⁽¹⁹⁾ B.N. Ratcliff,⁽²⁹⁾ T.W. Reeves,⁽³⁷⁾ J. Reidy,⁽¹⁸⁾ P.L. Reinertsen,⁽³⁵⁾
 P.E. Rensing,⁽²⁹⁾ L.S. Rochester,⁽²⁹⁾ P.C. Rowson,⁽⁹⁾ J.J. Russell,⁽²⁹⁾ O.H. Saxton,⁽²⁹⁾
 T. Schalk,⁽³⁵⁾ R.H. Schindler,⁽²⁹⁾ B.A. Schumm,⁽³⁵⁾ J. Schwiening,⁽²⁹⁾ S. Sen,⁽⁴⁰⁾
 V.V. Serbo,⁽²⁹⁾ M.H. Shaevitz,⁽⁹⁾ J.T. Shank,⁽⁶⁾ G. Shapiro,⁽¹⁵⁾ D.J. Sherden,⁽²⁹⁾
 K. D. Shmakov,⁽³²⁾ C. Simopoulos,⁽²⁹⁾ N.B. Sinev,⁽²²⁾ S.R. Smith,⁽²⁹⁾ M. B. Smy,⁽¹⁰⁾
 J.A. Snyder,⁽⁴⁰⁾ H. Staengle,⁽¹⁰⁾ A. Stahl,⁽²⁹⁾ P. Stamer,⁽²⁸⁾ H. Steiner,⁽¹⁵⁾
 R. Steiner,⁽¹⁾ M.G. Strauss,⁽¹⁷⁾ D. Su,⁽²⁹⁾ F. Suekane,⁽³³⁾ A. Sugiyama,⁽²¹⁾
 S. Suzuki,⁽²¹⁾ M. Swartz,⁽¹⁴⁾ A. Szumilo,⁽³⁸⁾ T. Takahashi,⁽²⁹⁾ F.E. Taylor,⁽¹⁹⁾
 J. Thom,⁽²⁹⁾ E. Torrence,⁽¹⁹⁾ N. K. Toumbas,⁽²⁹⁾ T. Usher,⁽²⁹⁾ C. Vannini,⁽²⁶⁾
 J. Va'vra,⁽²⁹⁾ E. Vella,⁽²⁹⁾ J.P. Venuti,⁽³⁷⁾ R. Verdier,⁽¹⁹⁾ P.G. Verdini,⁽²⁶⁾
 D. L. Wagner,⁽⁸⁾ S.R. Wagner,⁽²⁹⁾ A.P. Waite,⁽²⁹⁾ S. Walston,⁽²²⁾ J. Wang,⁽²⁹⁾
 S.J. Watts,⁽⁵⁾ A.W. Weidemann,⁽³²⁾ E. R. Weiss,⁽³⁸⁾ J.S. Whitaker,⁽⁶⁾ S.L. White,⁽³²⁾
 F.J. Wickens,⁽²⁷⁾ B. Williams,⁽⁸⁾ D.C. Williams,⁽¹⁹⁾ S.H. Williams,⁽²⁹⁾ S. Willocq,⁽¹⁷⁾
 R.J. Wilson,⁽¹⁰⁾ W.J. Wisniewski,⁽²⁹⁾ J. L. Wittlin,⁽¹⁷⁾ M. Woods,⁽²⁹⁾ G.B. Word,⁽³⁷⁾
 T.R. Wright,⁽³⁹⁾ J. Wyss,⁽²⁴⁾ R.K. Yamamoto,⁽¹⁹⁾ J.M. Yamartino,⁽¹⁹⁾ X. Yang,⁽²²⁾
 J. Yashima,⁽³³⁾ S.J. Yellin,⁽³⁴⁾ C.C. Young,⁽²⁹⁾ H. Yuta,⁽²⁾ G. Zapalac,⁽³⁹⁾
 R.W. Zdarko,⁽²⁹⁾ J. Zhou.⁽²²⁾

(The SLD Collaboration)

⁽¹⁾ *Adelphi University, South Avenue- Garden City, NY 11530,*

⁽²⁾ *Aomori University, 2-3-1 Kohata, Aomori City, 030 Japan,*

⁽³⁾ *INFN Sezione di Bologna, Via Irnerio 46 I-40126 Bologna (Italy),*

⁽⁵⁾ *Brunel University, Uxbridge, Middlesex - UB8 3PH United Kingdom,*

⁽⁶⁾ *Boston University, 590 Commonwealth Ave. - Boston, MA 02215,*

⁽⁷⁾ *University of Cincinnati, Cincinnati, OH 45221,*

⁽⁸⁾ *University of Colorado, Campus Box 390 - Boulder, CO 80309,*

⁽⁹⁾ *Columbia University, Nevis Laboratories P.O.Box 137 - Irvington, NY 10533,*

⁽¹⁰⁾ *Colorado State University, Ft. Collins, CO 80523,*

⁽¹¹⁾ *INFN Sezione di Ferrara, Via Paradiso, 12 - I-44100 Ferrara (Italy),*

⁽¹²⁾ *Lab. Nazionali di Frascati, Casella Postale 13 I-00044 Frascati (Italy),*

⁽¹³⁾ *University of Illinois, 1110 West Green St. Urbana, IL 61801,*

⁽¹⁵⁾ *Lawrence Berkeley Laboratory, Dept.of Physics 50B-5211 University of California-Berkeley, CA 94720,*

⁽¹⁶⁾ *Louisiana Technical University, ,*

⁽¹⁷⁾ *University of Massachusetts, Amherst, MA 01003,*

⁽¹⁸⁾ *University of Mississippi, University, MS 38677,*

⁽¹⁹⁾ *Massachusetts Institute of Technology, 77 Massachusetts Avenue Cambridge, MA*

02139,

(20) *Moscow State University, Institute of Nuclear Physics 119899 Moscow Russia,*

(21) *Nagoya University, Nagoya 464 Japan,*

(22) *University of Oregon, Department of Physics Eugene, OR 97403,*

(23) *Oxford University, Oxford, OX1 3RH, United Kingdom,*

(24) *Universita di Padova, Via F. Marzolo, 8 I-35100 Padova (Italy),*

(25) *Universita di Perugia, Sezione INFN, Via A. Pascoli I-06100 Perugia (Italy),*

(26) *INFN, Sezione di Pisa, Via Livornese, 582/AS Piero a Grado I-56010 Pisa (Italy),*

(27) *Rutherford Appleton Laboratory, Chiton, Didcot - Oxon OX11 0QX United Kingdom,*

(28) *Rutgers University, Serin Physics Labs Piscataway, NJ 08855-0849,*

(29) *Stanford Linear Accelerator Center, 2575 Sand Hill Road Menlo Park, CA 94025,*

(30) *Sogang University, Ricci Hall Seoul, Korea,*

(31) *Soongsil University, Dongjakgu Sangdo 5 dong 1-1 Seoul, Korea 156-743,*

(32) *University of Tennessee, 401 A.H. Nielsen Physics Blg. - Knoxville, Tennessee 37996-1200,*

(33) *Tohoku University, Bubble Chamber Lab. - Aramaki - Sendai 980 (Japan),*

(34) *U.C. Santa Barbara, 3019 Broida Hall Santa Barbara, CA 93106,*

(35) *U.C. Santa Cruz, Santa Cruz, CA 95064,*

(37) *Vanderbilt University, Stevenson Center, Room 5333 P.O. Box 1807, Station B Nashville, TN 37235,*

(38) *University of Washington, Seattle, WA 98105,*

(39) *University of Wisconsin, 1150 University Avenue Madison, WI 53706,*

(40) *Yale University, 5th Floor Gibbs Lab. - P.O. Box 208121 - New Haven, CT 06520-8121.*

Table 1: Contributions to the relative systematic error on A_P .

Error Source	$\delta A_P / A_P$
α_b	5.7%
Monte Carlo statistics on λ	1.0%
Tag Composition	3.9%
Detector Modeling	1.0%
Beam Polarization	0.8%
Total	7.1%

Figure Captions

Figure 1. P_t -corrected vertex mass distribution for (a) highest energy jets, (b) second-highest energy jets, and (c) lowest energy jets. The histograms are Monte Carlo simulations; the flavor compositions of the simulations are indicated.

Figure 2. Numbers of significant tracks in b-tagged events for (a) highest energy jets, (b) second-highest energy jets, and (c) lowest energy jets. The histograms are Monte Carlo simulations; the flavor compositions of the simulations are indicated.

Figure 3. Polar-angle distribution of the signed-thrust axis direction with respect to the electron-beam direction for (a) left-handed and (b) right-handed electron beam. The histograms are Monte Carlo estimations of the backgrounds.

Figure 4. Azimuthal-angle distribution of the signed-thrust axis direction with respect to the electron-beam direction for (a) left-handed and (b) right-handed electron beam. The histograms are Monte Carlo estimations of the backgrounds.

Figure 5. Left-right-forward-backward asymmetry in polar-angle distribution of the vector normal to the event plane for (a) CP-even case, and (b) CP-odd case. The solid curve is the best fit to the data sample, and the dashed curves correspond to the 95% C.L. limits.

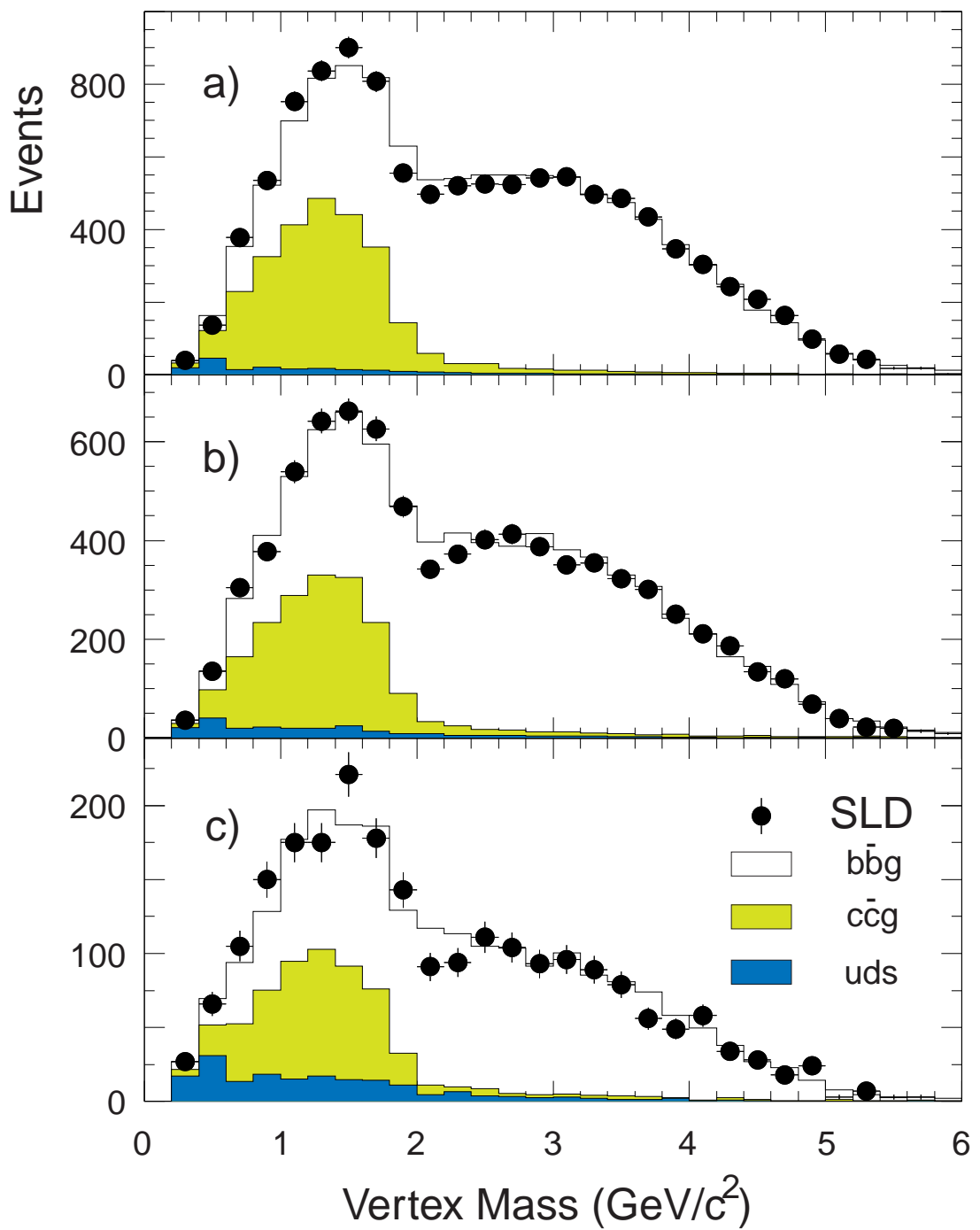


Figure 1

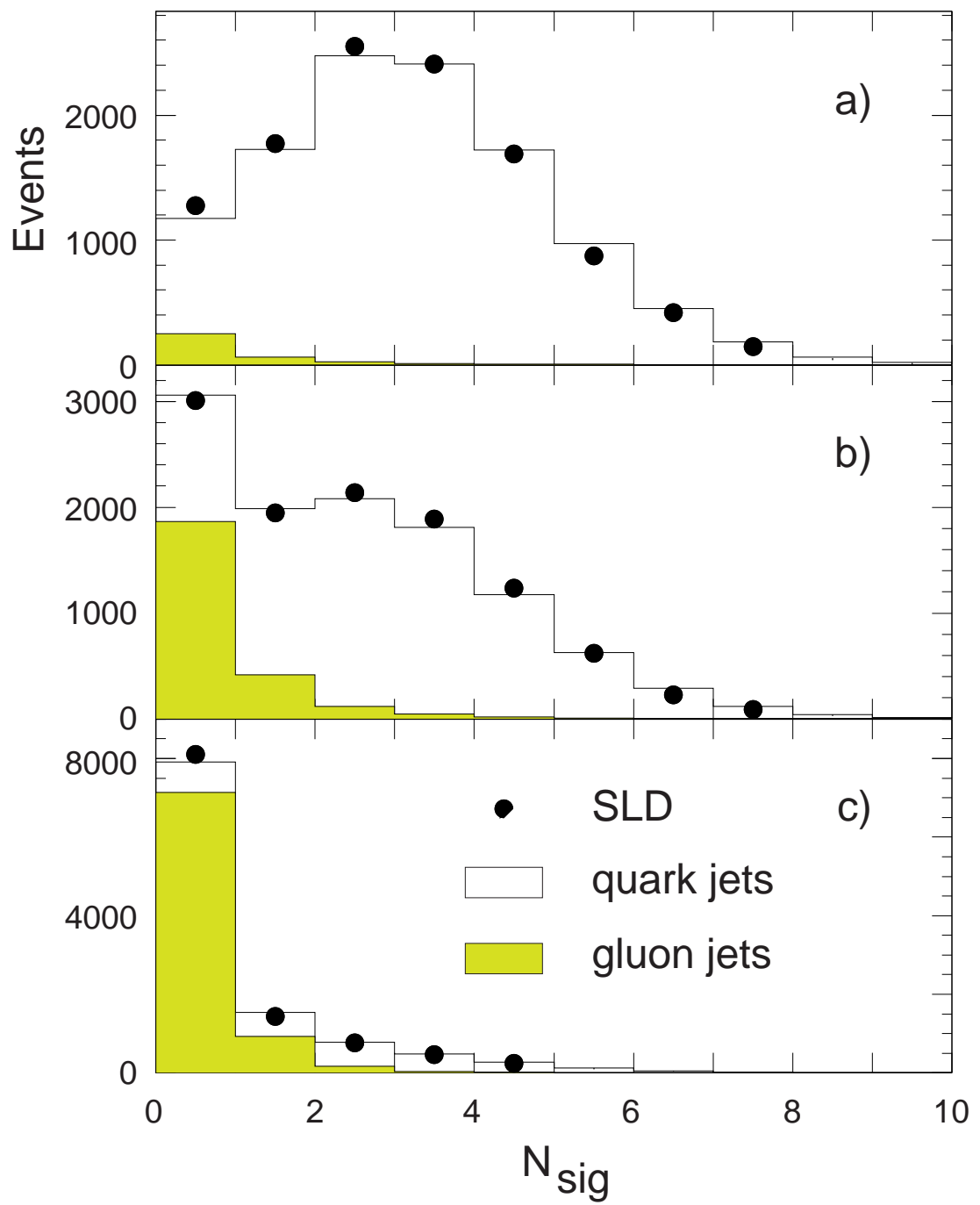
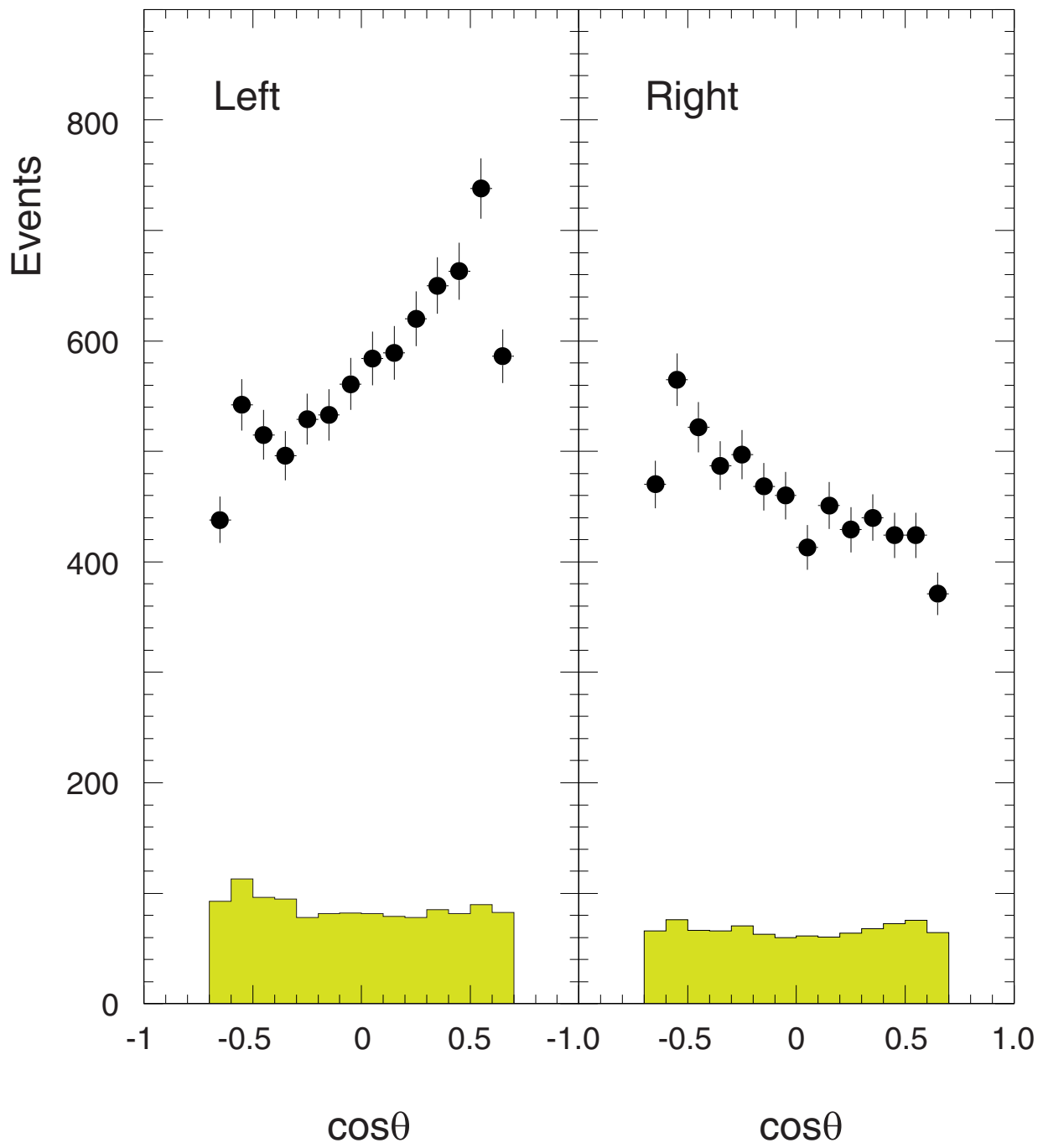


Figure 2

SLD Preliminary



SLD Preliminary

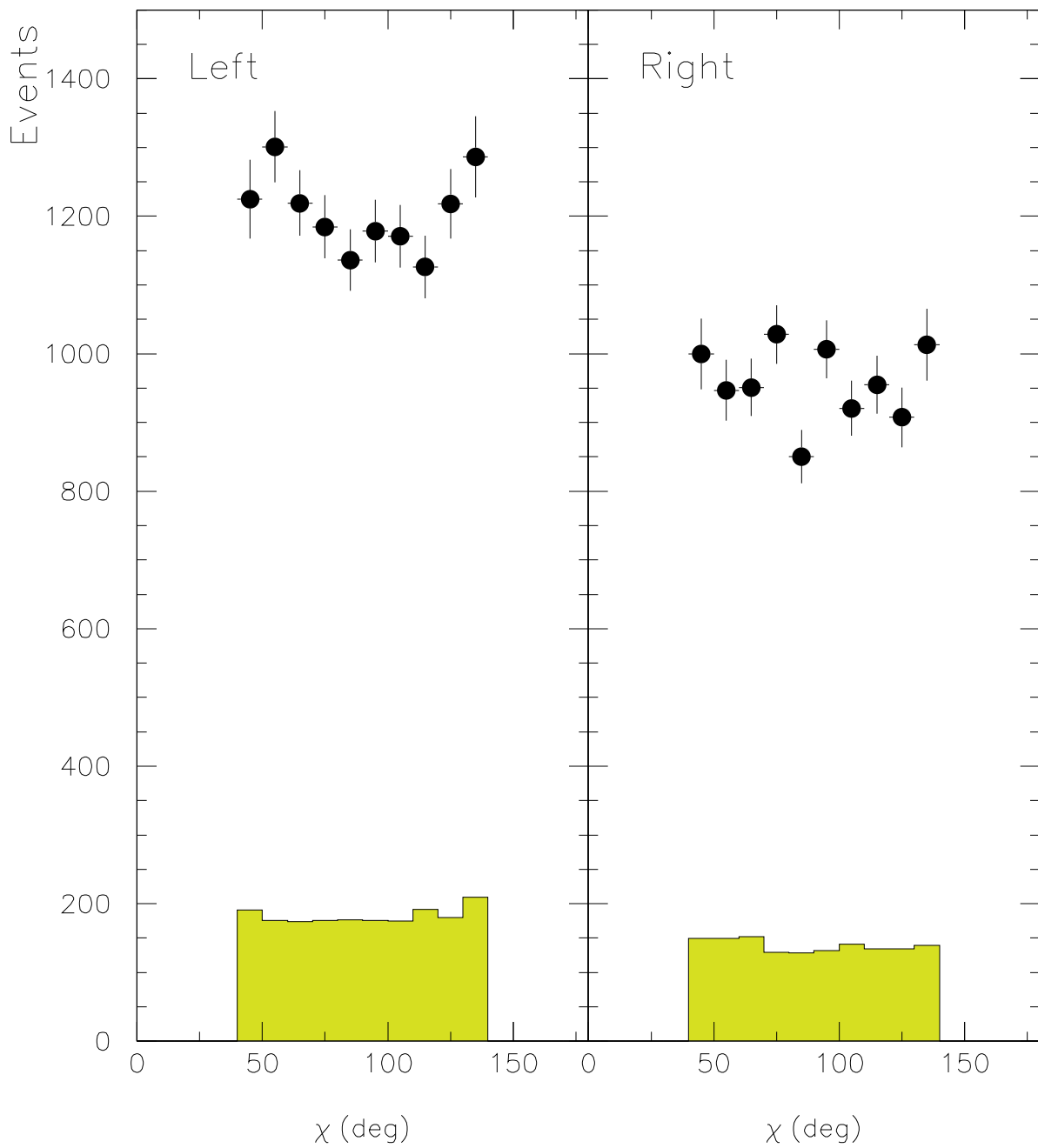


Figure 4

SLD Preliminary

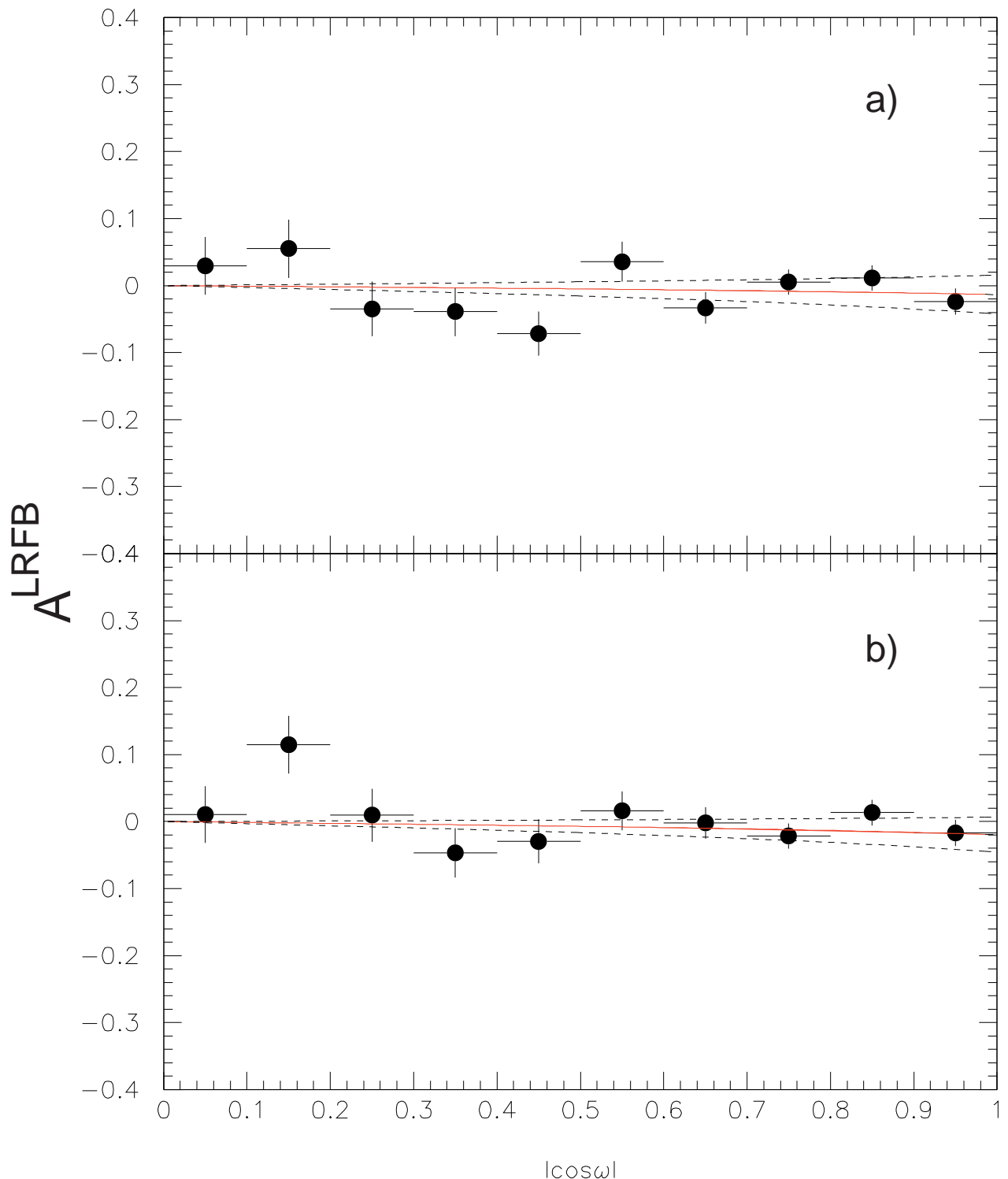


Figure 5